An energy-based model to predict wear in nanocrystalline diamond atomic force microscopy tips

R. Agrawal, N. Moldovan,[a] and H. D. Espinosa[b]
Department of Mechanical Engineering, Northwestern University, 2145 Sheridan Road, Evanston, Illinois 60208-3111, USA

(Received 9 July 2009; accepted 6 August 2009; published online 24 September 2009)

Atomic force microscopy (AFM) is one of the most powerful techniques to probe surfaces and material properties at the nanoscale, and pattern organic and inorganic molecules. In all cases, knowledge of the tip geometry and its evolution with continued use is essential. In this work, a broadly applicable energy model for the evolution of scanning probe tip radii during use is presented based on quantitative wear experiments. Experiments were conducted using AFM probes made of both undoped and nitrogen-doped diamond. Undoped diamond probes were found to be nearly ten times more wear resistant than commercially available silicon nitride probes. For a constant applied force, a linear relationship between wear volume and total dissipation energy is identified. The change in tip radius was also found to be proportional to the square root of scan distance, $x^{0.5}$.
 [doi:10.1063/1.3223316]

I. INTRODUCTION

In the past decade, the application of atomic force microscopy (AFM) to investigate surfaces at the nanoscale has increased significantly. The development of techniques to accurately control contact forces, applied by sharp cantilever probes, has made the AFM a very powerful imaging and surface analysis tool for nanoscale research. The resolution of the method is limited by the tip's sharpness, material, and geometry. Both the vertical and lateral resolutions continuously degrade during the scanning process as the probe tip wears and its contact diameter increases.[1] This tip degradation introduces artifacts in imaging, which leads to errors in step height measurements.[1,2] The wear of tip material during scanning also affects nanopatterning techniques, such as dip pen nanolithography,[3,4] nanofountain probe patterning,[5–9] and scanning probe contact printing,[10,11] as the size of patterned features depends on the radius of the tip. Knowing the extent of tip wear is also important for hardness measurements using AFM nanoindentation or atomic force acoustic microscopy,[12,13] as the interpretation of results depends on the tip radius.[14,15] Finally, characterization of wear is relevant to other AFM-based techniques such as nanografting[16–18] and scanning spreading resistance microscopy,[19] where very high contact forces are applied to displace the desired molecules from the substrate.

Ideally, an AFM tip with an infinitesimally small tip radius could exactly define the surface topography. However, real tips typically have finite radii, ranging from subnanometer to tens of nanometers. While images obtained with tips of finite radii lose some of the surface information, mathematical transformations can be performed to deconvolute the effect of tip shape and obtain accurate surface topography.[20,21] Unfortunately, retrieving the exact tip shape is as difficult as assessing the true geometry of a surface. Moreover, even if it is known with sufficient accuracy at one point in time, the tip geometry is subject to change due to continuous wear while scanning.

With this in mind, fabrication of AFM probes using extremely hard materials attracts continuous interest,[22] where low wear rates translate into a longer scanning life and consistent resolution. Diamond is among the hardest materials and is known for its extremely high mechanical strength and durability,[5,23,24] making it an attractive material for AFM probes. By exploiting the conformal properties of microwave plasma-enhanced deposition of ultrananocrystalline diamond (UNCD) thin films, AFM probes with superior performance have been fabricated.[5]

From a theoretical perspective, wear is a complex process involving a number of inelastic mechanisms. In general, for sliding wear, the volume of removed material is proportional to the dissipated energy and all the variable parameters are incorporated in constants called wear coefficients.[25] In earlier work, wear rates were usually quantified using Archard's approach in which the friction coefficient is assumed constant and the dissipated energy is proportional to the product of normal load, sliding distance, and friction coefficient.[25] Under such assumptions, the wear volume (V) is defined as

$$V = (k_{\mathrm{abr}} + k_{\mathrm{adh}})F_n L/H, \tag{1}$$

where F_n is the normal contact load, L is the sliding distance, and H is the hardness of material being removed. k_{abr} and k_{adh} are the wear coefficients for abrasion and adhesion, respectively. These wear coefficients are functions of the coefficient of friction, μ, and are typically determined experimentally. This simple formulation relates the wear volume to the amount of energy dissipated, i.e., the work done by the friction force ($\mu F_n L$).

At the macroscale, many researchers have proposed

[a]Present address: Advanced Diamond Technologies, Inc., Romeoville, IL 60466.
[b]Author to whom correspondence should be addressed. Electronic mail: espinosa@northwestern.edu.

similar "energy-based" models to predict wear rates validating them with experiments using a sliding tribometer or a ball-on-disk apparatus.[26,27] Several other tribological models have also been presented so far for various kinds of interacting surfaces.[28–31] Models relating dissipated energy to wear rates seem to be applicable at the macroscale; however, their direct applicability is not clear at the nanoscale as other forces (such as adhesive, capillarity, etc.) become prominent. Additionally, for single asperity contacts, Amanton's law does not necessarily hold and frictional forces are often not bound to be linearly proportional to the normal force.[32] D'Acunto and co-worker[33,34] proposed a diffusion based numerical model for quantification of adhesive/abrasive wear of an AFM probe tip and showed that one or the other mechanism can dominate based on the conditions of the tip and the substrate. To our knowledge, no broadly applicable model, based on experimental data, exists to predict evolution of AFM tips as scanning progresses.

In this work, the wear of monolithic doped and undoped UNCD AFM probes is experimentally quantified. Results are compared to conventionally used Si_3N_4 probes. Wear tests are performed under well-defined scanning conditions for the three probe materials. Tip shape and radius are characterized, by scanning electron microscopy (SEM) imaging, before and after wear to determine the volume of material lost during the process. Finally, a model is presented, which accurately predicts wear rates of AFM probes based on the total amount of energy dissipated during the process.

II. EXPERIMENTAL METHOD AND RESULTS

An AFM (Dimension 3100, Veeco Instruments) was used to perform wear tests using Si_3N_4 and UNCD (doped and undoped) probes by scanning them on the same substrate (composed of an UNCD film) for a given distance with a prescribed contact force. Commercial Si_3N_4 probes were purchased from Veeco Instruments (DNP Series). Doped UNCD probes were microfabricated using a process described in Ref. 5. Undoped UNCD probes were provided by Advanced Diamond Technologies, microfabricated using the molding process. The conductive diamond for the doped UNCD probes was *n*-type, obtained by microwave plasma-enhanced chemical vapor deposition from an $Ar-CH_4$ gas mixture with 10% nitrogen.[5] The spring constant of each individual probe used was measured by deflecting them against standard reference cantilevers (CLFC series, Veeco Instruments) with an established protocol.[35] Six cantilevers each of Si_3N_4 and undoped UNCD and three probes of doped UNCD were tested, the spring constants of which are summarized in Table I. The substrate used was an undoped UNCD film grown on a silicon wafer, with rms roughness of ~28.0 nm. In all the wear tests, contact mode scanning was performed in ambient conditions (temperature: 20°–30 °C; relative humidity: 25%–30%) at a scanning speed of 40 μm/s. Twelve scans of 5×5 μm^2 were performed with 512 lines per scan resulting in a total scan distance of 61.44 mm. The *applied* contact force (F_{app}) was varied from 70 to 280 nN to examine its effect on the wear rate. After every two scans, the tip was retracted and re-engaged to ensure that the applied contact load remained the same and no significant drift in the position of the laser spot occurred. The total contact force at any instant during the scan was calculated by including contributions from (i) applied contact force, (ii) surface tension force due to meniscus formation, and (iii) adhesion forces due to van der Waals type solid-solid interaction.

TABLE I. Measured stiffnesses (in N/m) of different AFM probes used for the wear tests.

Case No.	Si_3N_4	Doped UNCD	Undoped UNCD
1	0.122 ± 0.010	0.172 ± 0.014	0.032 ± 0.003
2	0.118 ± 0.007	⋯	0.083 ± 0.004
3	0.331 ± 0.019	⋯	0.182 ± 0.012
4	0.342 ± 0.027	0.194 ± 0.009	0.168 ± 0.014
5	0.579 ± 0.031	⋯	0.323 ± 0.023
6	0.561 ± 0.042	0.397 ± 0.021	0.342 ± 0.029

The volume of material lost from the AFM tips during scanning was calculated based on the initial and final tip geometries. The tip geometry was characterized by two different approaches: (i) direct imaging by SEM, and (ii) applying a mathematical algorithm[21] to deconvolute the effect of tip radius, such that the roughness of a given substrate can be used to predict the tip radius. The details of the mathematical method (MM) are provided in the electronic physics auxiliary publication service (EPAPS) supplementary material (Sec. 1).[36] Both methods agree reasonably well in measuring the tip radii; however, the applicability of MM is limited. The MM is found to fail when the radius of the tip was larger than the autocorrelation length of the substrate. A table comparing the tip radii obtained via SEM observation and MM prediction is provided in the EPAPS supplementary material (Table S1).[36] Figure 1 shows SEM images of probes before and after wear at an applied contact force of 70 nN. From the initial and final tip radii, the amount of volume removed during wear is calculated from the geometrical parameters as described in the EPAPS supplementary material (Sec. 2).[36] Table II summarizes the applied contact loads and measured wear volumes for the three different probe materials. In addition to the tip, the wear of the substrate was also investigated by AFM scanning using a previously unworn tip. AFM images (see EPAPS supplementary material, Sec. 3)[36] revealed negligible substrate wear, as there were no noticeable changes in the topography. The negligible wear of the substrate can be attributed mainly to the fact that during a scan, any point on the substrate establishes contact with the tip just once.

III. A DISSIPATED ENERGY-BASED MODEL TO PREDICT WEAR

The total dissipated energy (E) in the tip is calculated by integrating the frictional force (F_{fr}) acting on the tip over the entire scan distance, L, as $E=\int_0^L F_{fr}(x)dx$. The frictional force is related to the interfacial shear strength (τ) and the contact area (A_c) between the tip and the substrate as $F_{fr}=\tau A_c$. The interfacial shear strength (τ) depends on the tip and substrate material and is assumed to be a constant.[32] The experimental

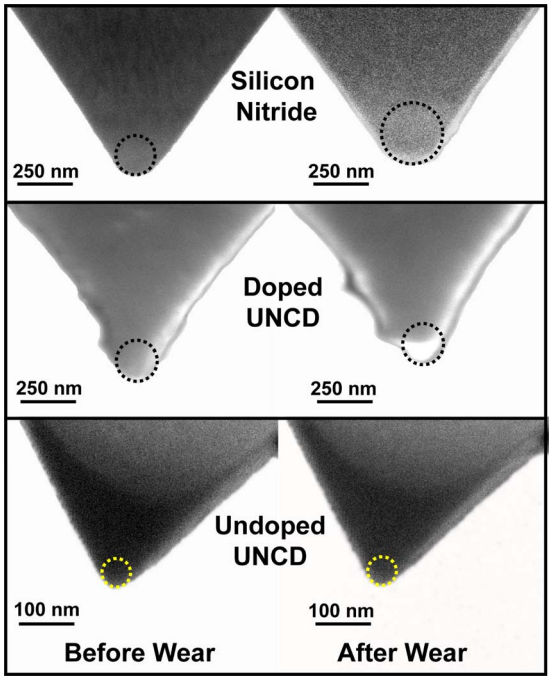

FIG. 1. (Color online) SEM images of Si_3N_4, doped UNCD, and undoped UNCD probes before and after wear at a contact force of ~70 nN (scan velocity=40.0 μm/s, scan distance=61.44 mm, and humidity =25%–30%).

measurement of τ in our experiments is discussed later. The contact area $A_c = \pi a^2$, where a is the contact radius. For single asperity contact, a is calculated based on Derjaguin–Muller–Toporov (DMT) theory[37] as

$$a = \left(\frac{3F_n R}{4Y^*}\right)^{1/3}, \tag{2}$$

where R is the radius of the tip, F_n is the total normal contact load, and Y^* is the reduced Young's modulus for the tip-substrate system. The DMT approximation is used, rather than the Johnson–Kendall–Roberts[38] or Maugis–Dugdale[39] theory of adhesion, in view that tip and substrate in this study are made of hard materials; namely, silicon nitride and diamond. The use of the DMT model is consistent with the findings of Xu *et al.*,[40] who reported that the DMT theory is applicable in AFM experiments for a broad range of humidity levels.

As mentioned earlier, the adhesion and meniscus forces, prominent at the nanoscale, are accounted for in the calculation of total normal load. The total normal load (F_n) is given by the sum of the applied contact force (F_{app}), the meniscus force (F_{men}), and the adhesion force (F_{adh}), i.e.,

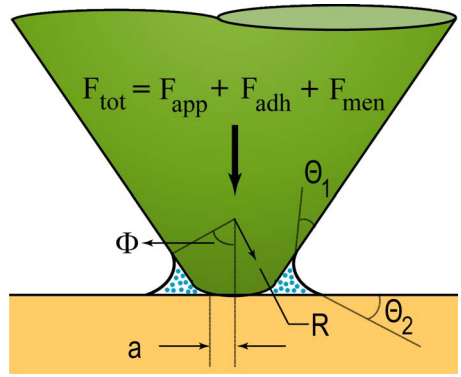

FIG. 2. (Color online) Schematic of an AFM probe showing all the forces contributing to the total normal contact load.

$$F_n = F_{app} + F_{men} + F_{adh}. \tag{3}$$

Figure 2 schematically shows the forces contributing to the total normal load and the various parameters used in their calculation. The applied force is determined by the deflection of the AFM cantilever and its stiffness, and is given in Table II for different cases. The total pull-off forces obtained for each tip represented the sum of F_{men} and F_{adh}. The meniscus force arises due to the condensation of water vapor around the area of contact in humid environments. F_{men} is a function of humidity and tip radius and is calculated as[41]

$$F_{men} = \pi\gamma_L R\left(\frac{\cos(\theta_1+\Phi)+\cos(\theta_2)}{\delta/R+1-\cos\Phi}\sin^2\Phi - \sin\Phi\right) + 2\pi\gamma_L R\sin\Phi\sin(\theta_1+\Phi), \tag{4}$$

where R is the tip radius, γ_L is the surface tension of water, θ_1 and θ_2 are the contact angles of water with tip and substrate, respectively, Φ is the wetting angle, and δ is the thickness of the water layer between the tip and the substrate. As the applied contact loads in our study are always greater than 70 nN, the contact stresses are well above 20 MPa, which is the critical stress needed to squeeze out the water monolayer between the tip and the substrate.[42,43] Therefore, under this condition, $\delta=0$ and Φ reduces to zero. Hence, the meniscus force can be approximated by its upper bound given by

TABLE II. Volume of material removed as observed experimentally for Si_3N_4 and UNCD probes.

Case No.	Applied contact force (nN)	Wear Volume (V) ($\times 10^5$ nm^3)		
		Si_3N_4	Doped UNCD	Undoped UNCD
1	70 ± 3.5	5.12 ± 1.21	0.08 ± 0.06	0.02 ± 0.01
2	100 ± 5	27.6 ± 3.91	···	2.17 ± 0.87
3	130 ± 6.5	42.6 ± 2.22	···	5.64 ± 1.62
4	175 ± 8.5	176 ± 6.71	30.6 ± 4.86	10.3 ± 2.36
5	200 ± 10	345 ± 10.6	···	15.7 ± 2.79
6	280 ± 14	887 ± 74.9	102 ± 8.78	32.5 ± 7.54

$$F_{\text{men}} = 2\pi\gamma_L R(\cos\theta_1 + \cos\theta_2). \quad (5)$$

The adhesion force is calculated based on the DMT (Ref. 37) theory of adhesion

$$F_{\text{adh}} = 2\pi w R, \quad (6)$$

where w is the work of adhesion for a given tip-substrate pair.

From the total pull-off forces, F_{men} and F_{adh} can be separately calculated using the initial tip radius, the surface tension of water ($\gamma_L = 73\ \text{mJ/m}^2$), and the contact angles (see EPAPS supplementary information Sec. 4 for further details).[36] The separation of the meniscus and adhesion forces is not relevant for the model presented later, but it provides a way to quantify the work of adhesion (w). Contact angles, measured using VCA Optima contact angle measurement equipment, on flat geometries were found to be $39.5° \pm 1.6°$ for Si_3N_4, and $66.0° \pm 2.1°$ for doped and undoped UNCD. The values for work of adhesion (w) (Refs. 32 and 44) were found to be 88.2 ± 6.7, 71.8 ± 5.0, and $66.0 \pm 5.8\ \text{mJ/m}^2$ for Si_3N_4, doped UNCD, and undoped UNCD probes, respectively. This quantitative assessment of w is subjected to the assumption that the contact angles measured on flat surfaces also hold for the geometry at the nanoscale.

As the total normal load during the scan is a function of tip radius, we assume the following nonlinear variation for the tip radius as a function of scanning distance, x:

$$R = R_i + (R_f - R_i)\left(\frac{x}{L}\right)^m, \quad (7)$$

where R_i and R_f are the initial and final tip radii after scanning a distance L, and m (ranging between 0 and 1) is an exponent to be determined by fitting the experimental data. From Eq. (7), the rate of change in the tip radius as the scan progresses can be obtained by differentiation

$$\frac{dR}{dx} = \frac{m}{L^m}(R_f - R_i)x^{m-1}. \quad (8)$$

As the tip wears, its radius increases and contact stresses decrease [contact stress σ is proportional to (F_n/a^2), and, from Eq. (2), it can be deduced that σ varies as $R^{-1/3}$]. This means that the rate of further change in radius should be decreasing. This imposes a constraint on m, namely, $m < 1$.

From Eqs. (2)–(7), the contact radius (a) can be calculated as a function of scan distance x and the total energy dissipated found by integration, namely,

$$E = \int_0^L F_{\text{fr}} dx = \int_0^L \tau\pi a^2(x) dx. \quad (9)$$

In order to calculate the interfacial strength (τ), the frictional force was measured[45] at different contact loads (and therefore different contact areas). The slope of the frictional force versus contact area plot defined the interfacial strength, which was found to be constant for each tip-substrate material pair within the experimental error (see EPAPS supplementary information Sec. 5 for details). For these measurements, the contact loads were kept low (<20 nN) to avoid any wear and maintain the same tip radius throughout these measurements. The interfacial strengths were found to be 343, 277, and 198 MPa for Si_3N_4, doped UNCD, and undoped UNCD probes, respectively, against the undoped UNCD substrate. The constant interfacial strength observed in our experiments is in agreement with the micromechanical dislocation model of frictional slip reported by Hurtado and Kim.[46,47] They asserted that below a critical value (~14 nm) for the contact radius, as is the case for most of the AFM experiments, the interfacial strength is a constant. Recently, they reported that a micrometer-scale asperity with nanometer-scale roughness exhibits a single asperity such as response of friction,[48] which also validates our calculations for contact radius based on single asperity contact. Our experimental results are also in agreement with the work of Xu *et al.*,[49] who reported a transition in interfacial shear strength from several hundreds of MPa to several tens of MPa over a 20–30 nm range of contact radii. Last, the assumption of constant interfacial strength even at larger contact loads is justified by the predictions of model, which agrees quite well with the experimental findings.

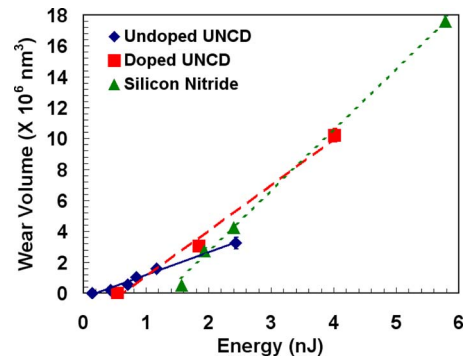

FIG. 3. (Color online) Dissipated energy vs wear volume for three different probe materials. The error bars are within the size of dots used for plotting the experimental data.

The wear volume for different values of the exponent m was plotted against the total energy dissipated (E) given by Eq. (9). A linear fit was obtained for different values of m; however, the best regression coefficient of >99% was obtained with $m = 0.5$ for all material pairs (Fig. 3). This value of m is in agreement with the value reported by Maw *et al.*[50] for tribochemical wear of Si_3N_4 probes; however, they expressed the change in tip height $\sim(F_n t)^{0.5}$.

The experimentally identified linear relationship between dissipated energy and wear volume holds as long as the tip shape remains parabolic and the single asperity contact assumption applies. Therefore, the above analysis for silicon nitride probes was restricted to the cases with applied contact load <200 nN, where the tip retained its parabolic shape. For doped and undoped UNCD probes, the tip shape always remained parabolic. Accordingly, the wear volume (V) is given by

$$V = C_1 E + C_2, \quad (10)$$

where C_1 and C_2 are the slopes and intercepts of the linear fits. Table III summarizes the coefficients of linear fits to the experimental data.

TABLE III. Slope and intercepts of linear fits obtained for different probe materials.

Tip material	C_1 (nm^3/pJ)	C_2 (nm^3)	C_1^{-1} (GPa)	Y (GPa)[a]	$-C_2/C_1$ (pJ)
Silicon nitride	11 990	-8.32×10^6	82	310	705
Doped UNCD	6 733	-2.00×10^6	147	940	304
Undoped UNCD	3 277	-0.371×10^6	303	1050	116

[a]References 24, 54, and 55.

Assuming an ideal scenario of defect-free material at the nanoscale, at 0 K one would expect the onset of wear when stresses approach the theoretical strength. Based on this hypothesis, C_1^{-1} should dimensionally represent the theoretical strength of the material, σ_{th}. In general, σ_{th} is proportional to Young's modulus (Y) and lies between $Y/\pi - Y/8$.[51] Quantitatively, the values for C_1^{-1} (Table III) lie in that range for all the studied materials. Furthermore, by substituting $V=0$ in Eq. (10), we find that the energy dissipated in the absence of wear is $(-C_2/C_1)$, which can be associated with the energy dissipated in overcoming adhesion and in moving the meniscus. The $(-C_2/C_1)$ ratio, for each tip material, follows the same trend as the experimentally measured values of "work of adhesion" (w), which qualitatively represent the energy needed to overcome adhesion. These trends are very important because they reveal the physics of the wear process and can be used to formulate and interpret atomistic models.

From the linear relationship between dissipated energy and wear volume confirmed by our experimental data for the three different probe materials, we propose a general methodology to predict the wear evolution of AFM tips. The wear rate can be expressed as the first derivative of Eq. (10) with respect to scan distance

$$\frac{dV}{dx} = C_1\frac{dE}{dx} = C_1 F_{fr} = C_1 \tau \pi a^2(x). \tag{11}$$

By performing experiments under well-defined scanning and environmental conditions, constants C_1 and C_2 can be determined for a given tip-substrate system. For an initial tip radius and applied contact load, the contact radius can be determined and therefore the wear rate calculated from Eq. (11). Using a discrete numerical integration scheme, the tip radius at the end of each incremental scan distance Δx can be calculated from the wear volume at the end of the step. A simple algorithm based on this methodology can be used to predict the tip radius at any instant during the scan, as follows.

(1) Measure the initial tip radius (R_i), applied force (F_{app}), and the tip shape.
(2) Initialize the scan distance, $x=0$; define $R_x=R_i$.
(3) Calculate F_{men} and F_{adh} from R_x and other material properties, using Eqs. (5) and (6).
(4) Calculate contact radius (a), using Eqs. (2) and (3).
(5) Calculate instantaneous wear rate ($\Delta V/\Delta x$) using Eq. (11).
(6) For an incremental scan distance (Δx), calculate wear volume (ΔV).
(7) Calculate tip radius at the end of incremental scan distance ($R_{x+\Delta x}$) from the shape of the tip [e.g., for a pyramidal tip, the wear volume (V) is related to initial and final tip radii by $V=\pi/3(R_{x+\Delta x}{}^3 - R_x{}^3)\Theta$].
(8) Increment $x(x=x+\Delta x)$; redefine the initial tip radius, $R_x=R_{x+\Delta x}$.
(9) Repeat steps 3–8 until $x=L$, where L is the total scan distance.
(10) Calculate the final radius $R_f=R_{x+\Delta x}$ at the end of scan.

We used this procedure to assess the performance of diamond tips when compared to silicon nitride ones. For an initial tip radius ranging from 5 to 80 nm and an applied contact force of 70 nN, we integrated Eq. (11) and calculated that doped and undoped UNCD probes can scan ~15 and ~4 times more distance than Si_3N_4 probes for the same amount of wear. These figures of merit are based on the wear tests against a hard UNCD substrate; however, such quantification is also possible for other softer substrates (such as metals, polymers, etc.) by employing the appropriate contact mechanics theory. Additionally, it is important to point out that the results presented here are for a constant scan velocity. Nonetheless, the model presented could be extended to include velocity dependence by calculating $dV/dt = (v\,dV/dx)$, where v is the scan velocity. This implies linear velocity dependence as opposed to the logarithmic dependence reported earlier[52,53] at very low velocities and low contact forces. The prediction of linear dependence might be reasonable for the velocity and force regimes investigated in this work. An experimental verification of this generalization is to be pursued in future work.

IV. FINAL REMARKS

This work quantified wear of AFM tips made of doped and undoped UNCDs and identified the improvement in wear resistance when diamond is employed in microfabrication of AFM probes. Comparing UNCD to Si_3N_4, an order of magnitude improvement in wear resistance is identified. In the case of doped UNCD, the nitrogen doping added during film deposition, to yield electrically conductive probes, leads to a slight decrease in wear resistance. This is consistent with the degradation in mechanical properties (elasticity, strength, and fracture toughness) measured in undoped and doped UNCD thin films.[54] The findings reported here assert that diamond qualifies as the material of choice for AFM probes.

An energy-based model and an experimental methodology are presented to predict the wear degradation of tips as a function of dissipated energy. Experiments are performed to achieve a *characteristic curve* relating wear volume to the dissipated energy. After identifying such characteristic for a

given tip-substrate system, the tip evolution can be estimated if the initial tip radius and the scanning conditions are known.

ACKNOWLEDGMENTS

This work was supported by the Nanoscale Science and Engineering Initiative of the National Science Foundation under NSF Award No. EEC-0647560 and through Grant Nos. NSF-NIRT-0304472 and CMMI-0555734. The authors acknowledge use of the fabrication and characterization facilities of the Center for Nanomaterials (CNM) at Argonne National Laboratory and Cornell Nanoscale Facility (CNF), a member of the National Nanotechnology Infrastructure Network, which is supported by the National Science Foundation (Grant No. ECS-0335765). N.M. also acknowledges the support of NSF-STTR Grant No. 0638030.

[1]E. Meyer, H. J. Hug, and R. Bennewitz, *Scanning Probe Microscopy: The Lab on a Tip* (Springer, Berlin, 2003).
[2]H. Edwards, R. McGlothlin, and E. U, J. Appl. Phys. **83**, 3952 (1998).
[3]J. Haaheim, R. Eby, M. Nelson, J. Fragala, B. Rosner, H. Zhang, and G. Athas, Ultramicroscopy **103**, 117 (2005).
[4]D. S. Ginger, Angew. Chem. **43**, 30 (2004).
[5]K.-H. Kim, N. Moldovan, C. Ke, H. D. Espinosa, X. Xiao, J. A. Carlisle, and O. Auciello, Small **1**, 866 (2005).
[6]K.-H. Kim, R. G. Sanedrin, A. M. Ho, S. W. Lee, N. Moldovan, C. A. Mirkin, and H. D. Espinosa, Adv. Mater. **20**, 330 (2008).
[7]B. Wu, A. M. Ho, N. Moldovan, and H. D. Espinosa, Langmuir **23**, 9120 (2007).
[8]N. Moldovan, K.-H. Kim, and H. D. Espinosa, J. Micromech. Microeng. **16**, 1935 (2006).
[9]N. Moldovan, K.-H. Kim, and H. D. Espinosa, J. Microelectromech. Syst. **15**, 204 (2006).
[10]X. Wang, K. S. Ryu, D. A. Bullen, J. Zou, H. Zhang, C. A. Mirkin, and C. Liu, Langmuir **19**, 8951 (2003).
[11]H. Li, D.-J. Kang, M. G. Blamire, and W. T. S. Huck, Nano Lett. **2**, 347 (2002).
[12]D. C. Hurley, M. Kopycinska-Muller, and A. B. Kos, J. Miner. Met. Mater. Soc. **59**, 23 (2007).
[13]D. Passeri, A. Bettucci, M. Germano, M. Rossi, A. Alippi, S. Orlanducci, M. L. Terranova, and M. Ciavarella, *Effect of Tip Geometry on Local Indentation Modulus Measurement Via Atomic Force Acoustic Microscopy Technique* (AIP, New York, 2005), p. 093904.
[14]L. Calabri, N. Pugno, A. Rota, and S. Valeri, J. Phys.: Condens. Matter **19**, 395002 (2007).
[15]N. Pugno, Acta Mater. **55**, 1947 (2007).
[16]S. Xu, S. Miller, P. E. Laibinis, and G. Liu, Langmuir **15**, 7244 (1999).
[17]J.-F. Liu, S. Cruchon-Dupeyrat, J. C. Garno, J. Frommer, and G.-Y. Liu, Nano Lett. **2**, 937 (2002).
[18]Q. Tang, S.-Q. Shi, and L. Zhou, J. Nanosci. Nanotechnol. **4**, 948 (2004).
[19]S. M. Kluth, D. Álvarez, St. Trellenkamp, J. Moers, S. Mantl, J. Kretz, and W. Vandervorst, J. Vac. Sci. Technol. B **23**, 76 (2005).
[20]P. Markiewicz and M. C. Goh, J. Vac. Sci. Technol. **13**, 1115 (1995).
[21]J. S. Villarrubia, J. Res. Natl. Inst. Stand. Technol. **102**, 425 (1997).
[22]V. Blank, M. Popov, N. Lvova, K. Gogolinsky, and V. Reshetov, J. Mater. Res. **12**, 2952 (1997).
[23]C. Mihalcea, W. Scholz, A. Malave, D. Albert, W. Kulisch, and E. Oesterschulze, Appl. Phys. A: Mater. Sci. Process. **66**, 87 (1998).
[24]H. D. Espinosa, B. Peng, N. Moldovan, T. A. Friedmann, X. Xiao, D. C. Mancini, O. Auciello, J. Carlisle, C. A. Zorman, and M. Merhegany, Appl. Phys. Lett. **89**, 073111 (2006).
[25]E. Rabinowicz, *Friction and Wear of Materials*, 2nd ed. (Wiley, New York, 1995).
[26]P. Gautier and K. Kato, Wear **162–164**, 305 (1993).
[27]A. Ramalho and J. C. Miranda, Wear **260**, 361 (2006).
[28]B. Bhushan, *Handbook of Nanotechnology*, 2nd ed. (Springer, Berlin, 2007).
[29]B. Bhushan, *Nanotribology and Nanomechanics: An Introduction* (Springer, Berlin, 2005).
[30]B. Bhushan, *Introduction to Tribology* (Wiley, New York, 2002).
[31]B. Bhushan, J. N. Israelachvili, and U. Landman, Nature (London) **374**, 607 (1995).
[32]*Handbook of Micro/Nano Tribology*, The Mechanics and Materials Science Series, 2nd ed., edited by B. Bhushan (CRC, Boca Raton, FL, 1999).
[33]M. D'Acunto, Nanotechnology **15**, 795 (2004).
[34]R. Bassani and M. D'Acunto, Tribol. Int. **33**, 443 (2000).
[35]C. T. Gibson, S. Myhra, and G. S. Watson, Nanotechnology **7**, 259 (1996).
[36]See EPAPS supplementary material at http://dx.doi.org/10.1063/1.3223316. Section 1 describes the MM used to predict the tip radius based on the surface roughness. Section 2 describes the calculation of wear volume. Section 3 illustrates that the wear of the surface was negligible. Section 4 describes the separation of meniscus and adhesive forces from the measured pull-off forces. Section 5 asserts the linear dependence of frictional force on contact area in our measurements.
[37]B. V. Derjaguin, V. M. Muller, and Y. P. Toporov, J. Colloid Interface Sci. **53**, 314 (1975).
[38]K. L. Johnson, K. Kendall, and A. D. Roberts, Proc. R. Soc. London **324**, 301 (1971).
[39]D. Maugis, J. Colloid Interface Sci. **150**, 243 (1992).
[40]D. Xu, K. M. Liechti, and K. Ravi-Chandar, J. Colloid Interface Sci. **315**, 772 (2007).
[41]X. Xiao and L. Qian, Langmuir **16**, 8153 (2000).
[42]R. M. Pashley and J. N. Israelachvili, J. Colloid Interface Sci. **101**, 511 (1984).
[43]A. M. Homola, J. N. Israelachvili, P. M. McGuiggan, and M. L. Gee, Wear **136**, 65 (1990).
[44]J. N. Israelachvili, *Intermolecular and Surface Forces*, 2nd ed. (Academic, New York, 1991).
[45]J.-A. Ruan and B. Bhushan, Trans. ASME, J. Appl. Mech. **116**, 378 (1994).
[46]J. A. Hurtado and K.-S. Kim, Proc. R. Soc. London, Ser. A **455**, 3363 (1999).
[47]J. A. Hurtado and K.-S. Kim, Proc. R. Soc. London, Ser. A **455**, 3385 (1999).
[48]Q. Li and K.-S. Kim, Proc. R. Soc. London, Ser. A **464**, 1319 (2008).
[49]D. Xu, K. Ravi-Chandar, and K. M. Liechti, J. Colloid Interface Sci. **318**, 507 (2008).
[50]W. Maw, F. Stevens, S. C. Langford, and J. T. Dickinson, J. Appl. Phys. **92**, 5103 (2002).
[51]J. J. J. Mecholsky, Mater. Lett. **60**, 2485 (2006).
[52]E. Riedo, E. Gnecco, R. Bennewitz, E. Meyer, and H. Brune, Phys. Rev. Lett. **91**, 084502 (2003).
[53]E. Gnecco, R. Bennewitz, T. Gyalog, C. Loppacher, M. Bammerlin, E. Meyer, and H. J. Guntherodt, Phys. Rev. Lett. **84**, 1172 (2000).
[54]B. Peng, C. Li, N. Moldovan, H. D. Espinosa, X. Xiao, O. Auciello, and J. A. Carlisle, J. Mater. Res. **22**, 913 (2007).
[55]J. T. Paci, T. Belytschko, and G. C. Schatz, Phys. Rev. B **74**, 184112 (2006).